Journal of Catalysis 277 (2011) 95–103

Contents lists available at ScienceDirect

Journal of Catalysis

journal homepage: www.elsevier.com/locate/jcat

Hydroxyls-induced oxygen activation on "inert" Au nanoparticles for low-temperature CO oxidation

Kun Qian [a,b,c], Wenhua Zhang [b,d], Huaxing Sun [c], Jun Fang [a,b,c], Bo He [e], Yunsheng Ma [c], Zhiquan Jiang [a], Shiqiang Wei [e], Jinlong Yang [a,c,*], Weixin Huang [a,b,c,*]

[a] Hefei National Laboratory for Physical Sciences at the Microscale, University of Science and Technology of China, Jinzhai Road 96, Hefei 230026, China
[b] CAS Key Laboratory of Materials for Energy Conversion, University of Science and Technology of China, Jinzhai Road 96, Hefei 230026, China
[c] Department of Chemical Physics, University of Science and Technology of China, Jinzhai Road 96, Hefei 230026, China
[d] Department of Materials Science and Engineering, University of Science and Technology of China, Hefei 230026, China
[e] National Synchrotron Radiation Laboratory, University of Science and Technology of China, Hefei 230029, China

ARTICLE INFO

Article history:
Received 16 August 2010
Revised 20 October 2010
Accepted 21 October 2010
Available online 20 November 2010

Keywords:
Au nanocatalysis
Low-temperature CO oxidation
Hydroxyls
Oxygen activation

ABSTRACT

The NaOH additive substantially enhances the catalytic activity of Au/SiO_2 catalyst inert in catalyzing CO oxidation at temperatures below 150 °C, and $Au/NaOH/SiO_2$ catalyst with a NaOH:Au atomic ratio of 6 is active at room temperature. Both the particle size distribution and the electronic structure of Au nanoparticles were found to be similar in Au/SiO_2 and $Au/NaOH/SiO_2$ catalysts, unambiguously proving that hydroxyls on "inert" Au nanoparticles can induce the activation of O_2 for CO oxidation at room temperature. The accompanying density functional theory (DFT) calculation results reveal the determining role of COOH(a) in hydroxyls-induced activation of O_2 on the Au(1 1 1) surface. Our results successfully elucidate the influence of hydroxyls on the intrinsic activity of Au nanoparticles in CO oxidation, providing novel insights into the role of hydroxyls in the catalytic activity of Au catalysts and advancing the fundamental understanding of oxidation reactions catalyzed by Au catalysts.

1. Introduction

Low-temperature CO oxidation catalyzed by supported Au catalysts has received extensive investigations since Haruta et al. [1] first reported that ultrafine Au nanoparticles supported on metal oxides catalyze CO oxidation at temperatures as low as 203 K. In addition to CO oxidation, supported Au catalysts also exhibit unusual activity and selectivity in a wide array of reactions, particularly in catalytic reactions involving molecular oxygen [2]. Therefore, it is hoped that a thorough understanding of the apparently simple CO oxidation could serve as a platform to understand other oxidation reactions catalyzed by Au catalysts. Great strides have been made in the fundamental understanding of the system; however, there still remain several unresolved issues, particularly with respect to the nature of active site, the activation of oxygen, and the reaction mechanism [3–10].

Interestingly, moisture in the feed stream has been found to exert great influences on the Au-catalyzed low-temperature CO oxidation [11–25], and a mechanism for CO oxidation catalyzed by supported Au catalysts involving OH was firstly proposed by Bond and Thompson [26]. Daté et al. [13] reported that the moisture enhances the catalytic activity of Au/TiO_2, Au/Al_2O_3, and Au/SiO_2 in CO oxidation at 273 K for no less than two orders of magnitude and that the effect of moisture depends on the type of metal oxide support. They considered that H_2O chemisorbs on the support surface, facilitating the activation of oxygen and the decomposition of carbonate on the Au–metal oxide interface. Kung et al. [14–16] investigated in detail the promotion effect of H_2O or H_2 in the reaction mixture on Au/Al_2O_3 for low-temperature CO oxidation and proposed that the active site of Au/Al_2O_3 for low-temperature CO oxidation is an ensemble of Au^+–OH^- and Au(0) atoms. Adsorbed CO can insert into the Au^+–OH^- bond to form hydroxycarbonyl. The hydroxycarbonyl is then either oxidized to bicarbonate followed by the decarboxylation to Au^+–OH^- and CO_2 or decarboxylated to CO_2 and Au–H, in which the latter is oxidized to Au^+–OH^-. Sanchez-Castillo et al. [17] reported that support-free Au-nanotubes in polycarbonate membranes exhibit catalytic activity of CO oxidation at room temperature and that the activity is enhanced by liquid H_2O and further promoted by increasing the pH of the solution, which provides compelling evidence that the promotion effect of H_2O and hydroxyl (OH) groups can occur without the involvement of oxide supports. They [18] also reported the catalytic activity in CO oxidation at room temperature in aqueous solutions of polyoxometalates over carbon-supported Au nanoparticles that are catalytically inactive in gas-phase CO oxidation at room temperature. The underlying mechanism of the enhancement

* Corresponding authors at: Department of Chemical Physics, University of Science and Technology of China, Jinzhai Road 96, Hefei 230026, China. Fax: +86 551 3600437 (W. Huang), +86 551 3602969 (J. Yang).
E-mail addresses: jlyang@ustc.edu.cn (J. Yang), huangwx@ustc.edu.cn (W. Huang).

0021-9517/$ - see front matter © 2010 Elsevier Inc. All rights reserved.
doi:10.1016/j.jcat.2010.10.016

effect of H_2O on the catalytic activity of supported Au catalysts in low-temperature CO oxidation has also been studied by means of surface science studies of model catalysts [27–29]. Kim et al. [27] reported that impinging $C^{16}O$ on a Au(1 1 1) surface populated with atomic oxygen [^{16}O] and oxygen-labeled water [$H_2{}^{18}O$] at low surface temperatures produces both $C^{16}O^{16}O$ and $C^{16}O^{18}O$, indicating the direct involvement of water in CO oxidation. On the basis of combined experimental and theoretical calculation results, they [28] further proposed the following reaction mechanism of water-enhanced low-temperature CO oxidation on atomic-oxygen-covered Au(1 1 1): H_2O(a) reacts with O(a) to form OH(a) on Au(1 1 1) followed by the reaction of OH(a) with CO(a) to form CO_2. They also pointed out that more than one reaction pathways are involved in the oxidation of CO on Au(1 1 1) with coadsorbed oxygen adatoms and water.

Although the enhancement effect of H_2O on the activity of supported Au catalysts in low-temperature CO oxidation has been unambiguously identified, it remains as a challenging issue whether H_2O plays a role in the crucial oxygen activation step and how. No answer to this issue could be derived from previous reported systems [11–25], in which supported Au catalysts can catalyze the low-temperature CO oxidation and thus can activate oxygen without the addition of H_2O in the feed stream. Meanwhile, surface science studies of model catalysts all started from the atomic-oxygen-covered Au(1 1 1) surface, and thus the issue of oxygen activation was not involved [27–29]. Employing first-principle calculations, Bongiorno and Landman [30] revealed that a significant enhancement of the binding and activation of O_2 occurs upon the coadsorption of O_2 and H_2O on Au clusters supported on defect-free MgO(1 0 0) via the formation of a complex involving partial proton sharing or proton transfer. The activated O_2 in the complex consequently readily reacts with CO with a relatively low barrier. However, Liu et al. [31] employed DFT to study the role of H_2O in CO oxidation on Au/TiO_2(1 1 0), in which OH formed by H_2O adsorption on TiO_2 was found to facilitate the adsorption of O_2 on TiO_2, and then O_2(a) on TiO_2 could diffuse to the Au–TiO_2 interface to participate in CO oxidation. As far as we know, no experimental evidence has been reported to unambiguously demonstrate the role of H_2O in the oxygen activation step on supported Au catalysts.

We have recently investigated the effect of various additives on the structure and activity of Au/SiO_2 catalyst in CO oxidation [32–36]. The catalytic activity of Au nanoparticles supported on SiO_2 is much inferior to that of Au nanoparticles supported on "active" supports such as TiO_2 and CeO_2; however, the Au/SiO_2 catalyst has an advantage that SiO_2 does not contribute to the catalytic activity, greatly facilitating the elucidation of the intrinsic structure–activity relation of Au nanoparticles. In this paper, we report that the NaOH additive can induce the Au/SiO_2 catalyst inert in low-temperature CO oxidation to become active, proving that surface hydroxyls on "inert" Au nanoparticles can participate in the activation of O_2 for low-temperature CO oxidation. The accompanying DFT calculation results reveal a novel reaction mechanism of surface hydroxyls-induced low-temperature CO oxidation on the Au(1 1 1) surface, in which COOH(a), OOCOOH(a), and CO_3H(a) are the reaction intermediates.

2. Experimental section

Au/SiO_2 catalysts with a Au:SiO_2 weight ratio of 2% were prepared by traditional deposition–precipitation (DP) method employing $HAuCl_4$ as Au precursor [37]. Typically, 0.9017 g $HAuCl_4{\cdot}4H_2O$ (Sinopharm Chemical Reagent Co., Ltd., Au content $\geqslant$ 47.8%) was dissolved in 50 ml distilled water to prepare a 0.0438 mol L^{-1} $HAuCl_4$ aqueous solution. A volume of 11.59 ml $HAuCl_4$ aqueous solution, 5.0 g SiO_2 (40–120 mesh, Qingdao Haiyang Chemicals Co.), and 50 ml distilled water were co-added into a three-neck bottle and adequately mixed by stirring at 60 °C for 30 min. An appropriate amount of ammonium hydroxide was added to adjust the pH value of the system between 9 and 10, after which the system was stirred at 60 °C for 24 h. The solid was then filtered, washed with distilled water several times, dried at 60 °C for 12 h, and calcined at 200 °C for 4 h. The acquired Au/SiO_2 catalyst was then employed as the precursor for the preparation of Au/$NaOH/SiO_2$ catalysts by incipient wetness impregnation. One gram Au/SiO_2 catalyst was added to 2 ml NaOH aqueous solution containing calculated amounts of NaOH under stirring. The system was then adequately stirred and vacuum-dried at room temperature for 24 h, and finally calcined at 200 °C for 4 h.

The loadings of Au in Au/SiO_2 and Au/$NaOH/SiO_2$ catalysts were analyzed by an inductively coupled plasma atomic emission spectrometer (ICP-AES). Powder X-ray diffraction (XRD) patterns were acquired on a Philips X'Pert PRO SUPER X-ray diffractometer with a Ni-filtered Cu Kα X-ray source operating at 40 kV and 50 mA. X-ray photoelectron spectroscopy (XPS) measurements were performed on an ESCALAB 250 electron spectrometer using monochromatized Al Kα excitation source ($h\nu$ = 1486.6 eV). The binding energies in XPS spectra were referenced with respect to the C 1s binding energy of adventitious carbon at 284.5 eV. Transmission electron microscope (TEM) images were obtained on a JEOL 2010 transmission electron microscope. X-ray absorption spectroscopy (XAS) measurements for the Au L_{III}-edge (11,719–12,919 eV) were performed at room temperature on the XAS Station of the U7C beam line of National Synchrotron Radiation Laboratory (Hefei, China). The synchrotron radiation facility consists of an 800 MeV electron storage ring with the ring current of about 100–300 mA. A Si(1 1 1) double-crystal was used as the monochromator. X-ray absorption near edge structure (XANES) spectra was acquired at an energy step of 1 eV.

The catalytic activity was evaluated with a fixed-bed flow reactor. The catalyst experienced no pre-treatment prior to the catalytic reaction. The used catalyst weight was 100 mg, and the reaction gas consisting of 1% CO and 99% dry air was fed at a rate of 20 ml/min. The composition of the effluent gas was detected with an online GC-14C gas chromatograph equipped with a TDX-01 column (T = 80 °C, H_2 as the carrier gas at 30 ml/min). The steady-state conversion of CO was calculated from the change in CO concentrations in the inlet and outlet gases.

3. Theoretical calculations

Spin-polarization DFT calculations were performed with DMol^3 package [38]. Double-numeric quality basis set with polarization functions (DNP), DFT semi-core pseudopotential (DSPP), and PBE function [39] were used for all the atoms. A thermal smearing of 0.001 Hartree (Ha) and a real-space cutoff of 4.0 Å were adopted. In our calculations, the Au(1 1 1) surface was simulated with a four-layer-thick $p(3 \times 3)$ unit cell with ~15 Å vacuum space, and $3 \times 3 \times 1$ k-points sampling was used. All atoms except those in bottom two layers were relaxed. The adsorption energy of surface species was calculated according to $E_{ads} = (E_{surf} + E_{mole}) - E_{(surf+mole)}$, where E_{surf}, E_{mole}, $E_{(surf+mole)}$ represented the energy of surface, the energy of molecule or radical, and the total energy of adsorbed system, respectively. Synchronous transit methods [40] were used to find the transition states of each elementary step.

4. Results and discussion

Au/$NaOH/SiO_2$ catalysts with different NaOH:Au molar ratios were prepared and denoted as Au/$NaOH/SiO_2$-x (x denoting the

NaOH:Au molar ratio). The ICP-AES results demonstrate that the loading of Au in Au/NaOH/SiO_2 is similar with that in Au/SiO_2 (~1.8%). It is reasonable because Au/NaOH/SiO_2 catalysts were prepared employing Au/SiO_2 as the precursor. Fig. 1A shows the catalytic performance of various catalysts in CO oxidation. Au/SiO_2 exhibits poor catalytic activity, becoming active at reaction temperatures above 150 °C. The NaOH additive promotes the catalytic activity of Au/SiO_2, and the promotion effect depends on the NaOH:Au molar ratio in Au/NaOH/SiO_2 catalysts. The catalytic activity of Au/NaOH/SiO_2 improves remarkably with the initial increasing NaOH:Au molar ratio. Au/NaOH/SiO_2-6 is active in catalyzing CO oxidation at room temperature (30 °C), and the CO conversion reaches 30%, corresponding to a reaction rate of 0.0866 $mol_{CO}\ g_{Au}^{-1}\ h^{-1}$ under our reaction condition. With the further increasing NaOH:Au molar ratio, the catalytic activity of Au/NaOH/SiO_2 decreases. Fig. 1B compares T_{50} (the temperature corresponding to a 50% CO conversion) of various catalysts. Au/NaOH/SiO_2-6 is most active and achieves its $T_{50\%}$ at 320 K. The stability of Au/NaOH/SiO_2-6 in CO oxidation was also studied at different reaction temperatures, whose results are shown in Fig. 2. Au/NaOH/SiO_2-6 is quite stable at 90 °C but gradually deactivates at 60 °C. These results demonstrate that NaOH in Au/NaOH/SiO_2 is not consumed during the course of CO oxidation.

The XRD patterns of various catalysts (Fig. 3) do not show any differences, displaying diffraction peaks arising from Au nanoparticles. The particle size and size distribution of Au nanoparticles in Au/SiO_2, Au/NaOH/SiO_2-1, Au/NaOH/SiO_2-6, and Au/NaOH/SiO_2-10 were further investigated by TEM (Fig. 4). In all catalysts, Au nanoparticles were observed to be with a wide size distribution and their sizes are not finer than 4 nm. Fig. 5 shows the size distribution of Au nanoparticles in various catalysts counted from TEM images in Fig. 4. The average size of Au nanoparticles was calculated to be 7.2, 7.4, 7.1, and 8.0 nm in Au/SiO_2, Au/NaOH/SiO_2-1, Au/NaOH/SiO_2-6, and Au/NaOH/SiO_2-10, respectively. It can be clearly seen that the addition of NaOH does not change the size distribution of Au nanoparticles in the catalyst. This should be expected from the preparation method of Au/NaOH/SiO_2 catalysts, in which Au/SiO_2 calcined at 200 °C was employed as the precursor. Therefore, the enhanced activity of Au/NaOH/SiO_2 catalysts in CO oxidation, particularly the activity of Au/NaOH/SiO_2-6 at room temperature, should not result from the size effect of Au nanoparticles.

Fig. 6 shows the XPS spectra and the normalized C 1s XPS peak intensity of Au/SiO_2 and Au/NaOH/SiO_2 catalysts, and Table 1 summarizes the surface composition of these catalysts derived from

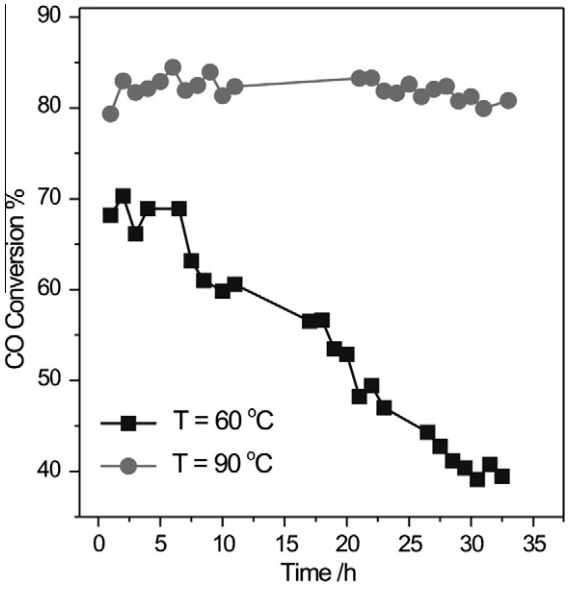

Fig. 2. Stability of Au/NaOH/SiO_2-6 in CO oxidation at different reaction temperatures.

the XPS results. The Si 2p and O 1s binding energy of all catalysts, respectively, locate at 103.1 and 532.4 eV, corresponding to Si and O in SiO_2 [41]. The Na 1s XPS spectra of Au/NaOH/SiO_2-*x* catalysts display a single peak with the binding energy at 1072.0 eV, a characteristic value for Na(I) cation [41]; its intensity strengthens with the increasing NaOH:Au atomic ratio. The addition of NaOH influences the carbon species and amount in the catalysts quite much. Only adventitious carbon with the binding energy at 284.5 eV appears in Au/SiO_2, and its surface atomic ratio is 7.03%. Comparing Au/SiO_2, the surface atomic ratio of carbon species increases to 14.46% in Au/NaOH/SiO_2-1, and besides the adventitious carbon, another C 1s XPS peak at 288.9 eV that could be assigned to carbonate [41] appears; meanwhile, the surface atomic ratio of Si and O decreases and that of Au slightly decreases. With the further increasing NaOH:Au atomic ratio in Au/NaOH/SiO_2 catalysts, the surface atomic ratio of carbon species keeps decreasing, and the C 1s XPS peak at 288.9 eV corresponding to carbonate gradually shifts to 288.4 eV that could be assigned to bicarbonate [41]. The formation of carbonate and bicarbonate could be due to the reaction between NaOH and CO_2 in the ambient condition, but it can

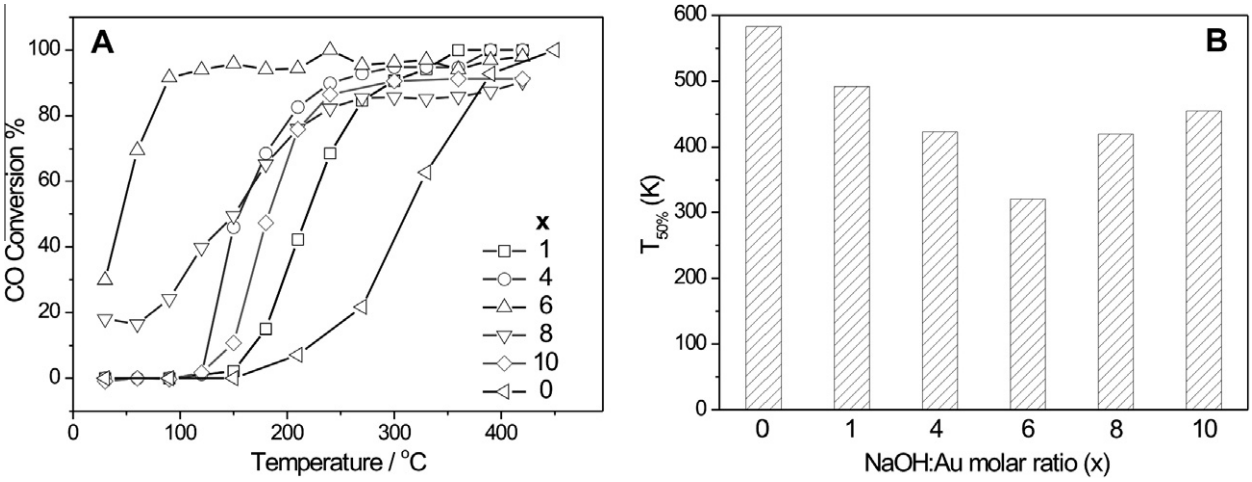

Fig. 1. Catalytic activity (A) and T_{50} (B) of various catalysts in CO oxidation.

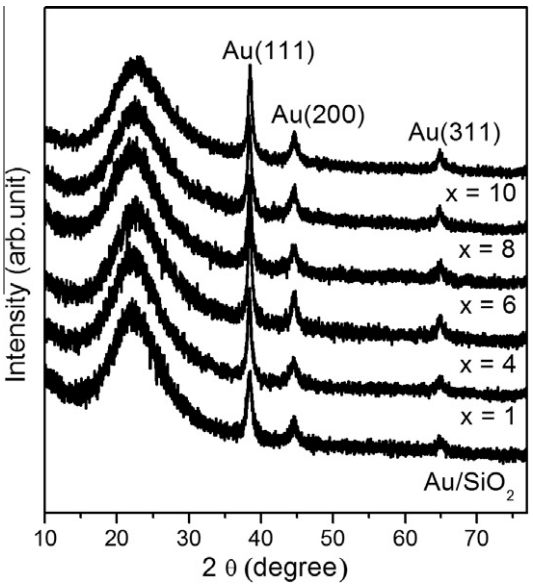

Fig. 3. XRD patterns of various catalysts.

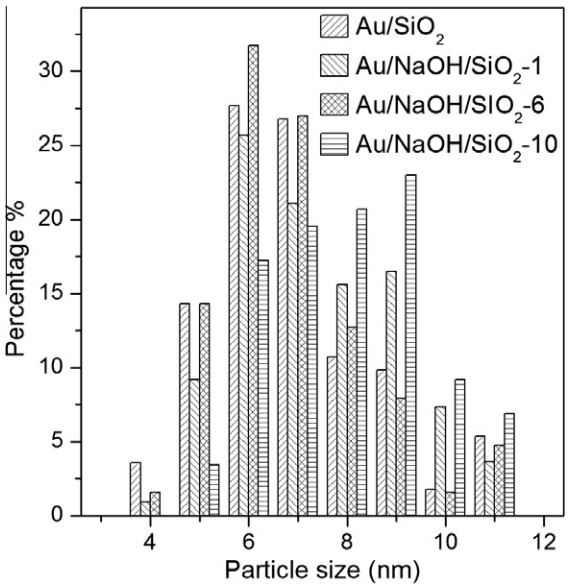

Fig. 5. Size distribution of Au nanoparticles in various catalysts.

be seen from Table 2 that the surface atomic ratio of carbonate and bicarbonate decreases with the increasing NaOH:Au atomic ratio in $Au/NaOH/SiO_2$ catalysts, which indicates that there might be some decomposition channels for carbonate and bicarbonate in the catalysts.

The Au 4f XPS spectra of all catalysts show a single component whose binding energy locates at 83.7 eV for $Au/NaOH/SiO_2$-x ($x \leqslant 6$) and slightly shifts to 83.5 eV for $Au/NaOH/SiO_2$-x ($x = 8$ and 10). This indicates that only metallic Au exists in all catalysts [41]. XAS was used to further probe the electronic structure of Au in Au/SiO_2 and $Au/NaOH/SiO_2$-6 (Fig. 7). The Au L_{III}-edge XANES spectra of Au/SiO_2 and $Au/NaOH/SiO_2$-6 are almost identical whose features can all be assigned to metallic Au [42]. The white-line peak in the spectrum of $Au/NaOH/SiO_2$-6 is slightly weaker than that of Au/SiO_2. This feature is due to a $2p_{3/2} \rightarrow 5d$ transition, and its intensity is proportional to the density of unoccupied d states and thus decreases with the reducing oxidation state of Au [43]. Therefore, both XANES and XPS results confirm that only metallic Au nanoparticles exist in Au/SiO_2 and $Au/NaOH/SiO_2$-x catalysts, but a weak charge transfer might occur from hydroxyls-derived surface adsorbates to Au nanoparticles in $Au/NaOH/SiO_2$.

Above structural characterization results clearly reveal that both the particle size distribution and the electronic structure of Au nanoparticles in $Au/NaOH/SiO_2$-x are similar to those in Au/SiO_2. However, $Au/NaOH/SiO_2$-x exhibits much better catalytic activity in CO oxidation than Au/SiO_2; moreover, $Au/NaOH/SiO_2$-6 is active in catalyzing CO oxidation at room temperature at which temperature Au/SiO_2 is completely inactive. Therefore, the activity of $Au/NaOH/SiO_2$-6 in low-temperature CO oxidation is induced by NaOH additives. It has been previously reported that Na(I) cation does not promote the activity of supported Au catalysts in CO oxidation [34,44], thus the promotion effect of NaOH on Au/SiO_2

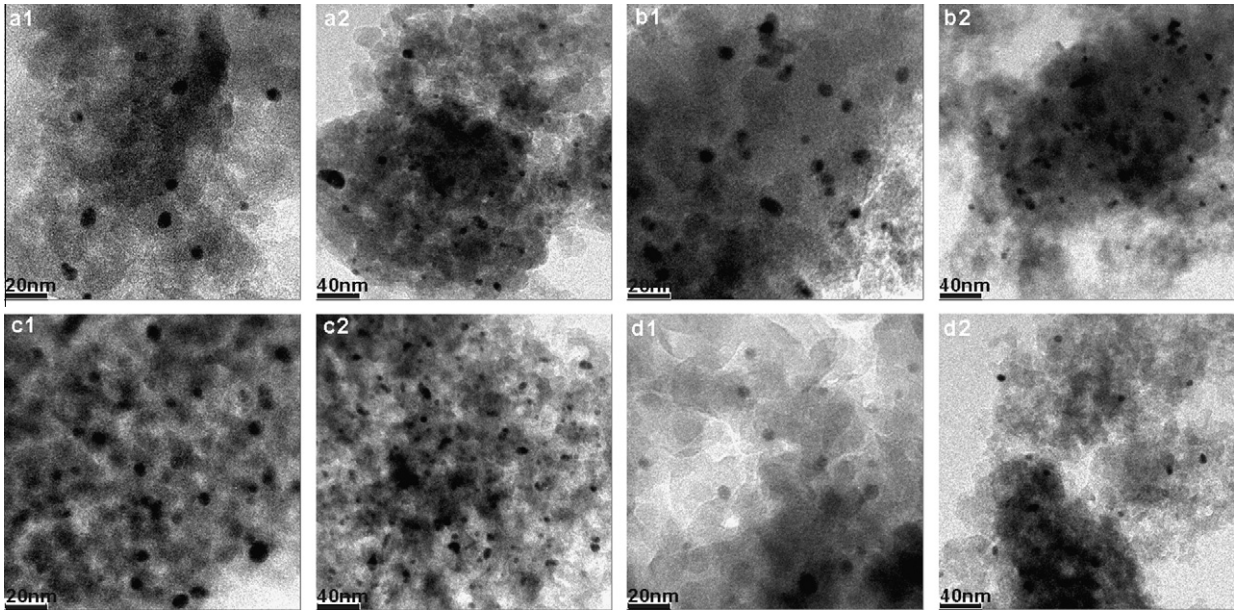

Fig. 4. Representative TEM images of Au/SiO_2 (a1 and a2), $Au/NaOH/SiO_2$-1 (b1 and b2), $Au/NaOH/SiO_2$-6 (c1 and c2), and $Au/NaOH/SiO_2$-10 (d1 and d2).

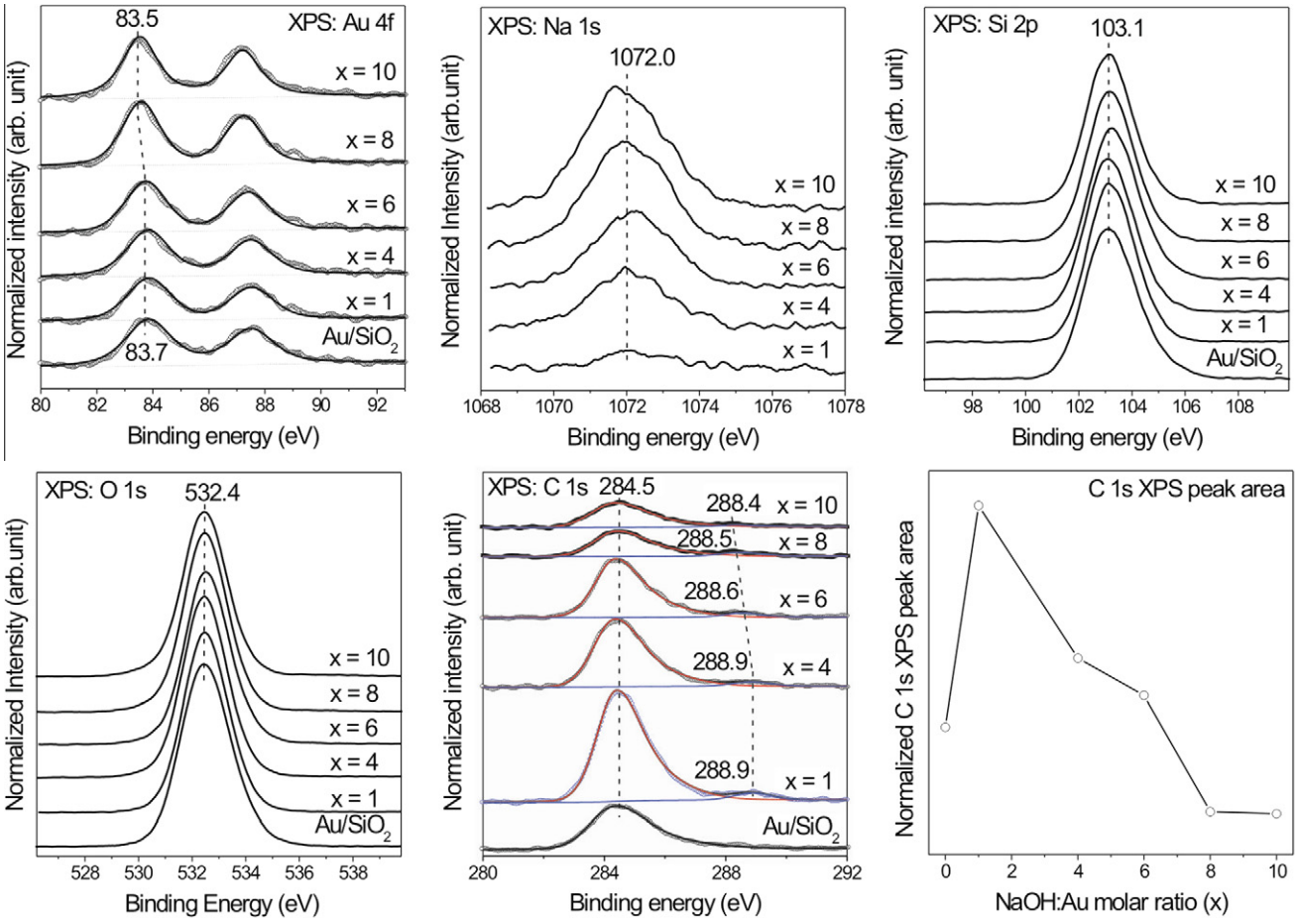

Fig. 6. Au 4f, Na 1s, Si 2p, O 1s, C 1s XPS spectra and the normalized C 1s XPS peak area of various catalysts.

Table 1
Surface compositions of Au/SiO2 and Au/NaOH/SiO2 catalysts derived from XPS results.

Catalyst	Atomic composition					
	Au	C		Na	Si	O
		Component 1[a]	Component 2[b]			
Au/SiO_2	0.10	7.03			22.53	70.35
$Au/NaOH/SiO_2$-1	0.09	13.95	0.51	0.45	20.62	64.29
$Au/NaOH/SiO_2$-4	0.10	9.16	0.33	1.40	21.67	67.31
$Au/NaOH/SiO_2$-6	0.11	7.95	0.41	1.78	22.23	67.41
$Au/NaOH/SiO_2$-8	0.13	4.11	0.33	2.53	22.44	70.26
$Au/NaOH/SiO_2$-10	0.13	3.79	0.26	3.10	22.57	70.06

[a] Adventitious carbon.
[b] Carbonate or bicarbonate.

comes from hydroxyl groups. SiO_2 is an inert support and does not participate in the catalytic reaction, thus the promotion effect can only occur on Au nanoparticles. Therefore, our results provide solid evidence that hydroxyls on "inert" Au nanoparticles supported on SiO_2 can induce their activity in low-temperature CO oxidation without the involvement of oxide support.

The enhancement effect of H_2O on the activity of supported Au catalysts in low-temperature CO oxidation has been unambiguously identified, in which hydroxyls have been proposed to play the key role [13–18]. It has also been clearly demonstrated that H_2O reacts with adsorbed oxygen atoms on Au(1 1 1) to form hydroxyl groups capable of reacting with CO at low surface temperatures to form CO_2 [27–29]. However, it is well known that the mechanism of molecular oxygen activation is one of the most challenging issues in the fundamental understanding of low-temperature CO oxidation catalyzed by supported Au catalysts. It also remains as a challenging issue whether H_2O plays a role in the crucial molecular oxygen activation step and how. No answer to this issue could be derived from the observed enhancement effect of H_2O in previous reported systems [11–25], in which supported Au catalysts can catalyze the low-temperature CO oxidation and thus can activate molecular oxygen even without the addition of H_2O in the feed stream. Meanwhile, surface science studies of model catalysts all started from the atomic-oxygen-covered Au(1 1 1) surface, and thus the issue of molecular oxygen activation was not involved [27–29]. With this respect, our results of SiO_2-supported Au catalysts provide novel and insightful experimental evidence. SiO_2 does not participate in the catalytic reaction, and Au/

Table 2
Activation energy and reaction enthalpy of elementary surface reactions on Au(1 1 1) considered in our calculations. Elementary surface reactions are divided into trigger, cycle, and poison steps.

	Elementary steps	E_a (eV)	ΔH (eV)
Trigger	OH(a) + CO(a) → COOH(a)	0.44	−1.15
Cycle 1	COOH(a) → CO_2(g) + H(a)	0.98	−0.54
	H(a) + O_2(g) → HO_2(a)	0.34	−0.42
	HO_2(a) → OH(a) + O (a)	0.57	−0.26
	CO(a) + O(a) → CO_2(g)	0.39	−2.55
Cycle 2	COOH(a) + O_2(g) → OOCOOH(a) (ring)	0.94	−0.81
	OOCOOH(a) → O(a) + *di*-CO_3H(a)	0.78	−0.87
	di-CO_3H(a) → *mono*-CO_3H(a)	0.60	+0.41
	mono-CO_3H(a) → OH(a) + CO_2(g)	0.39	+0.04
	CO(a) + O(a) → CO_2(g)	0.39	−2.55
	CO_2(g) + O(a) → CO_3(a)	0.79	+0.28
Poison	CO_3(a) → O (a) + CO_2(g)	0.51	−0.28
	CO_2(g) + OH(a) → *di*-CO_3H(a)	0.35	−0.45

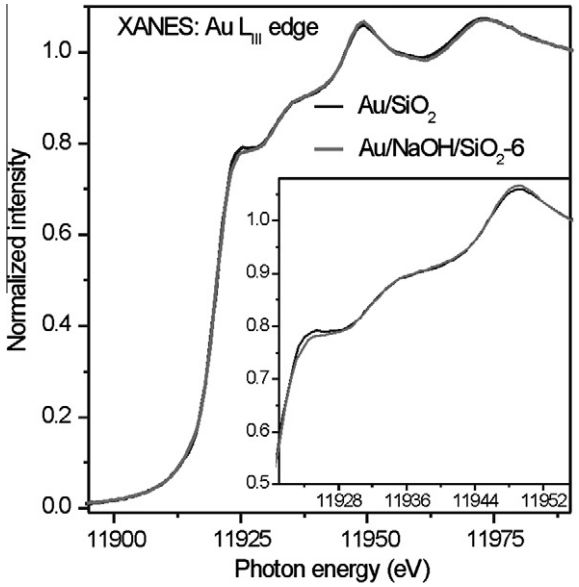

Fig. 7. Au L_{III} XANES spectra of Au/SiO_2 and $Au/NaOH/SiO_2$-6.

SiO_2 is completely inactive in CO oxidation at room temperature, demonstrating that Au nanoparticles in Au/SiO_2 are inert in activating molecular oxygen at room temperature. However, Au nanoparticles in $Au/NaOH/SiO_2$-6 with the similar particle size distribution and electronic structure to those in Au/SiO_2 are catalytically active in CO oxidation at room temperature, clearly demonstrating that hydroxyls can induce the activation of molecular oxygen on "inert" Au nanoparticles at room temperature. As far as we know, our results represent the first experimental evidence directly proving that hydroxyls on "inert" Au nanoparticles can activate molecular oxygen for low-temperature CO oxidation without the involvement of oxide supports. These results provide novel insights into the fundamental understanding of the intrinsic activity of Au nanoparticles in catalyzing oxidation reactions.

DFT theoretical calculations were performed to understand the hydroxyls-induced oxygen activation and catalytic activity of "inert" Au nanoparticles in low-temperature CO oxidation. Since Au nanoparticles themselves are inactive in activating molecular oxygen and catalyzing CO oxidation at room temperature, a Au(1 1 1) planar model, instead of a Au cluster model, was adopted to simulate Au nanoparticles in our catalysts. Water-enhanced low-temperature CO oxidation on O(a)-covered Au(1 1 1) has been experimentally observed [27,28], and relevant theoretical calculations have been performed employing O(a)-covered Au(1 1 1) as the model [28,45]. Ojifinni et al. [28] proposed the following mechanism: H_2O(a) reacts with O(a) to form OH(a) on Au(1 1 1) followed by the reaction of OH(a) with CO(a) to form CO_2. They also pointed out that more than one reaction pathways are involved in the oxidation of CO on Au(1 1 1) with coadsorbed oxygen adatoms and water. Our previous DFT calculation results [45] reveal another reaction pathway: CO(a) reacts with OH(a) on Au(1 1 1) to form COOH(a) with an activation energy of 0.44 eV, and COOH(a) dissociates to form gaseous CO_2 with a low activation barrier assisted by another H_2O(a). However, all these previous DFT calculations did not involve the crucial step of O_2 activation on Au(1 1 1) at all, and thus their results could not explain our current experimental results that hydroxyls can induce the activation of molecular oxygen on "inert" Au nanoparticles for CO oxidation at room temperature. Therefore, in our DFT calculations, we started with OH(a)-covered Au(1 1 1), CO, and O_2.

It is well known that the clean Au(1 1 1) surface is not able to adsorb and activate O_2. DFT theoretical calculation results have shown that coadsorption of H_2O can stabilize O_2(a) on Ag(1 1 1) to some extent [46]. However, our calculation results found neglectable influence of coadsorption of H_2O(a) or OH(a) on the adsorption energy of O_2 on Au(1 1 1), implying that H_2O(a) or OH(a) on Au(1 1 1) can not directly assist the adsorption and activation of O_2 on Au(1 1 1).

Our DFT calculation results reveal two likely reaction mechanisms for CO oxidation on OH(a)-covered Au(1 1 1), whose elementary surface reaction steps are summarized in Table 2. The elementary reaction steps were classified into trigger, cycle, and poison steps. The trigger step is the reaction of CO(a) with OH(a) to form COOH(a) on Au(1 1 1) that proceeds with an activation energy of 0.44 eV and a reaction enthalpy of −1.15 eV. The optimized geometric structure of COOH(a) on Au(1 1 1) is shown in Fig. 8a. Then, two catalytic oxidation mechanisms of COOH(a) on Au(1 1 1) by O_2 were found and schematically illustrated in Fig. 9. In mechanism I (Fig. 9a), COOH(a) firstly decomposes to CO_2 and H(a) on Au(111) with an activation energy of 0.98 eV and a reaction enthalpy of −0.54 eV, agreeing with previous DFT calculation results [28]. This suggests that COOH(a) on Au(1 1 1) is quite stable, in consistence with experimental observations that COOH(a) remains stable on Au(1 1 1) up to ~350 K [47]. Ojifinni et al. considered that the decomposition of COOH(a) on Au(1 1 1) with such a high activation barrier could not account for the H_2O-enhanced CO oxidation on O(a)-covered Au(1 1 1) below 180 K [28]. However, under the catalytic reaction conditions in our experiments ($T \geqslant 300$ K), we believe that this reaction can occur. The formed H(a) on Au(1 1 1) can readily react with O_2 to form HO_2(a) with an activation energy of 0.34 eV and a reaction enthalpy of −0.42 eV. The optimized geometric structure of HO_2(a) on Au(1 1 1) is shown in Fig. 8b. The formation of HO_2(a) by the reaction of O_2 with a single bridging OH group on TiO_2(1 1 0) has been recently identified by the combined STM and DFT studies [48,49]. This reaction is similar to the calculated first step of H_2O_2 synthesis from $H_2 + O_2$ on Au and AuPd surfaces [50]. HO_2(a) dissociates to OH(a) and O(a) on Au(1 1 1) with an activation energy of 0.57 eV and a reaction enthalpy of −0.26 eV, and O(a) then readily reacts with CO(a) to form CO_2. The calculated reaction path for the H(a) + O_2 reaction and the decomposition reaction of HO_2(a) on Au(1 1 1) is presented in Fig. 10. Therefore, the overall surface reaction of the cycle is 2CO(a) + O_2(g) + OH(a) → 2CO_2(g) + OH(a), and OH(a) acts as a cocatalyst. In this reaction mechanism, all the elementary surface reactions are exothermic, the rate-determining step is the decomposition of COOH(a), and the activation of O_2 is accomplished by its reaction with H(a) on Au(1 1 1). This reaction mechanism is similar to the water gas shift reaction mechanism

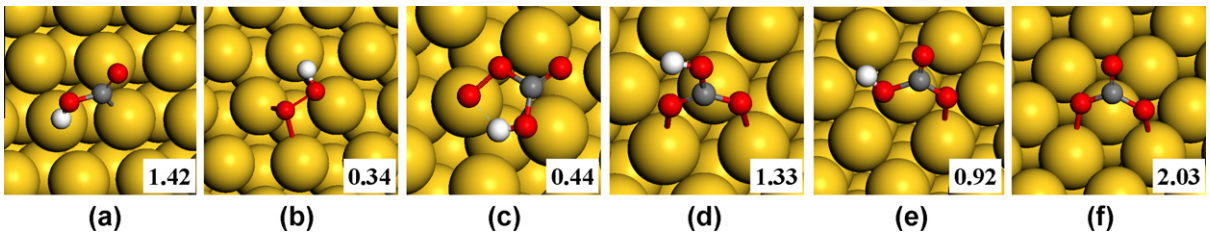

Fig. 8. Optimized geometric structures of important intermediates involved in surface reactions: (a) COOH, (b) HO_2, (c) ring-OOCOOH, (d) *di*-CO_3H, (e) *mono*-CO_3H, and (f) CO_3. The adsorption energy of each surface species is also shown.

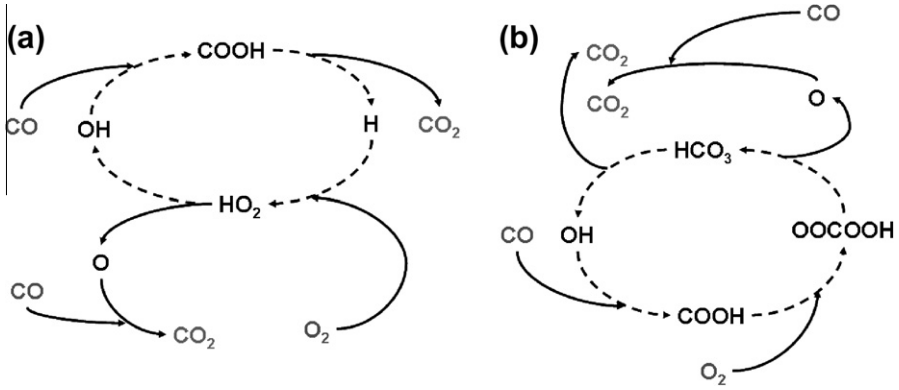

Fig. 9. Schematic illustrations of two different surface reaction cycles: (a) dissociation of COOH(a) and (b) reaction of COOH(a) with O2.

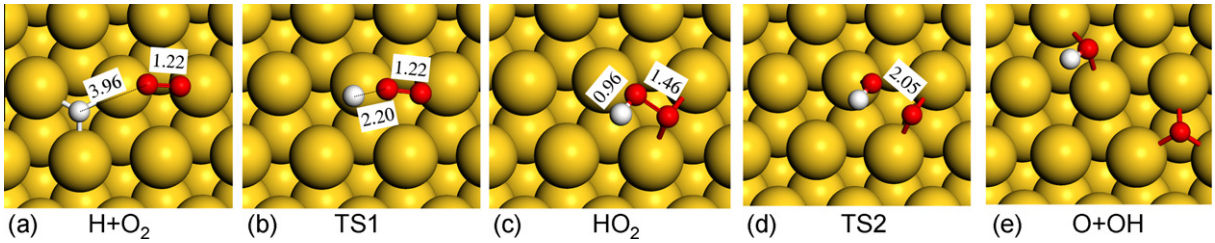

Fig. 10. Optimized geometric structures of initial state, transition state, and final state of elementary surface reaction of the formation of HO_2(a) by H(a) + O_2 and the decomposition of HO_2(a) to O(a) + OH(a) on Au(1 1 1).

catalyzed by TiO_{2-x}/Au(1 1 1) and CeO_{2-x}/Au(1 1 1) catalysts proposed by Rodriguez et al. [51]. In their reaction mechanism, CO(a) on Au(1 1 1) reacts with OH(a) on oxides at the Au–oxide interface to form COOH(a), COOH(a) decomposes to produce CO_2 and H(a), and H(a) then recombines to form H_2.

In mechanism II (Fig. 9b), COOH(a) reacts directly with O_2 to form OOCOOH(a) with a hydrogen-bonded five-membered ring structure on Au(1 1 1) with an activation energy of 0.94 eV and a reaction enthalpy of −0.81 eV. The optimized geometric structure of OOCOOH(a) on Au(1 1 1) is shown in Fig. 8c. Its ring structure is similar to the configuration of [CO_4] recently reported to be the intermediate of hyperthermal O-atom exchange reaction between O_2 and CO_2 [52]. OOCOOH(a) can undergo a decomposition reaction to form O(a) and *di*-CO_3H(a) with an activation energy of 0.78 eV and a reaction enthalpy of −0.87 eV. The optimized geometric structure of *di*-CO_3H(a) on Au(1 1 1) is shown in Fig. 8d, in which CO_3H(a) is bonded to Au(1 1 1) through two oxygen atoms. The calculated reaction path for the COOH(a) + O_2 reaction and the decomposition reaction of OOCOOH(a) on Au(1 1 1) is presented in Fig. 11. The formed O(a) reacts with

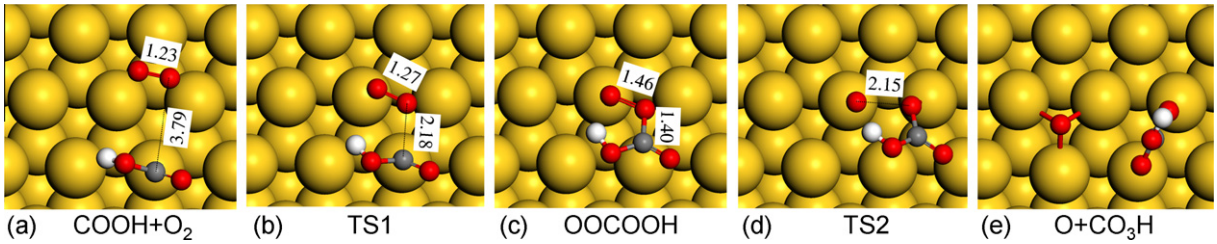

Fig. 11. Optimized geometric structures of initial state, transition state, and final state of elementary surface reaction of the formation of OOCOOH(a) by COOH(a) + O_2 and the decomposition of OOCOOH(a) to O(a) + CO_3H(a) on Au(1 1 1).

CO(a) to form CO_2. *di*-CO_3H(a) follows the reaction pathway schematically illustrated in Fig. 12: *di*-CO_3H(a) firstly transforms into *mono*-CO_3H(a) with an activation energy of 0.60 eV and a reaction enthalpy of 0.41 eV, and then *mono*-CO_3H(a) decomposes into CO_2 and OH(a) with an activation energy of 0.39 eV and a reaction enthalpy of 0.04 eV. Fig. 8e shows the optimized geometric structure of *mono*-CO_3H(a) bonded to Au(1 1 1) through one oxygen atom. Similar to mechanism I, the overall surface reaction of the cycle in mechanism II is $2CO(a) + O_2(g) + OH(a) \rightarrow 2CO_2(g) + OH(a)$, and OH(a) acts as a cocatalyst. In mechanism II, the transformation of *di*-CO_3H(a) into *mono*-CO_3H(a) and the decomposition of *mono*-CO_3H(a) into CO_2 and OH(a) are endothermic, other elementary surface reactions are exothermic. The rate-determining step is the reaction of COOH(a) with O_2 to form OOCOOH(a) on Au(1 1 1), which is also the activation step of O_2. Mechanism II is novel and has not been previously reported.

Above DFT calculation results demonstrate two complete reaction mechanisms for CO oxidation on OH(a)-covered Au(1 1 1) including the OH(a)-induced activation process of O_2. The activation energy of the rate-limiting step in both mechanisms is ~1 eV (96 kJ/mol). These theoretical calculation results adequately support the experimental results that the hydroxyls can induce the activation of O_2 on "inert" Au nanoparticles to catalyze CO oxidation at room temperature. Our results represent the first combined experimental and theoretical evidence for hydroxyls-induced oxygen activation on "inert" Au nanoparticles for low-temperature CO oxidation, providing novel insights into the role of hydroxyls in Au-catalyzed CO oxidation. On the basis of DFT theoretical calculations, two roles of H_2O/hydroxyls-enhanced catalytic activity of Au catalysts in CO oxidation have been previously proposed: one is to enhance the binding and activation of O_2 on Au clusters by the coadsorption of O_2 and H_2O [30] and the other is to facilitate the adsorption of O_2 on TiO_2 followed by the diffusion of O_2(a) to the Au–TiO_2 interface to participate in CO oxidation [31]. However, in both previously reported mechanisms, H_2O/hydroxyls only exhibit an enhancement effect because Au catalysts themselves can activate oxygen. However, in our mechanisms, hydroxyls act as a cocatalyst without which oxygen cannot be activated on the Au surface at room temperature. It is noteworthy that the activation energy of the rate-limiting elementary surface reactions reported in previous mechanisms [30,31] is ~0.5 eV, much lower than that in our case. Therefore, these different mechanisms might contribute to the activity of Au catalysts in CO oxidation at different reaction conditions. It has been generally accepted that CO oxidation catalyzed by Au catalysts proceeds with multireaction pathways. Moreover, the activation energy of elementary surface reactions in our mechanisms might reduce with the decrease in the size of supported Au nanoparticles.

It can be seen that the hydroxyls-induced CO oxidation is triggered by COOH(a) in our mechanisms. Kung et al. [14–16] have experimentally observed the formation of COOH(a) on Au/Al_2O_3 catalysts in CO oxidation in the presence of H_2O or H_2 in the reaction mixture. They [6] proposed that the active site of Au/Al_2O_3 in low-temperature CO oxidation is an ensemble of Au^+–OH^- together with Au(0) atoms and that COOH(a) formed by insertion of adsorbed CO into the Au^+–OH^- bond is the key reaction intermediate. COOH(a) is then either oxidized to bicarbonate followed by the decarboxylation to Au^+–OH^- and CO_2 or decarboxylated to CO_2 and Au–H, in which the latter is oxidized to Au^+–OH^-. Their mechanism is very similar to ours, but the dissociation of O_2 into O(a) on fine Au nanoparticles in Au/Al_2O_3 was assumed to be inevitable. Our current results demonstrate that such reaction mechanisms can occur exclusively on the "inert" Au surface without the participation of Au(I); moreover, COOH(a) can directly react with O_2 to initiate the catalytic reaction cycle.

Both reaction mechanisms that we calculated have the similar activation energy for the rate-limiting step, demonstrating that they should work simultaneously in the view of kinetics. However, in the view of thermodynamics, there are obvious differences between mechanisms I and II. In mechanism I, every elementary step is exothermic, implying that a low reaction temperature facilitates the oxidation of CO to CO_2 following mechanism I as long as the reaction temperature kinetically allows the occurrence of these elementary steps. However, in mechanism II, the transformation of *di*-CO_3H(a) into *mono*-CO_3H(a) and the decomposition of *mono*-CO_3H(a) into CO_2 and OH(a) are endothermic, whereas other elementary surface reactions are exothermic. This indicates that *di*-CO_3H(a) is thermodynamically favored and will accumulate on the surface at low reaction temperatures, which might eventually block mechanism II. Furthermore, we also found that the reaction product CO_2 can facilely react with hydroxyls to form *di*-CO_3H(a) on the Au(1 1 1) surface with an activation energy of 0.35 eV and a reaction enthalpy of −0.45 eV (Table 2). These results suggest that *di*-CO_3H(a) on the Au surface should be the poison that leads to the deactivation of Au catalysts in CO oxidation at low temperatures. On basis of this DFT calculation result, the experimentally observation that Au/NaOH/SiO_2-6 is deactivated at 60 °C but not at 90 °C could be attributed to the formation and accumulation of *di*-CO_3H(a) on the Au surface that is favored thermodynamically at low reaction temperatures. It is very interesting that the poisoning route for CO oxidation on OH(a)-covered Au(1 1 1) is thermodynamically controlled instead of kinetically controlled.

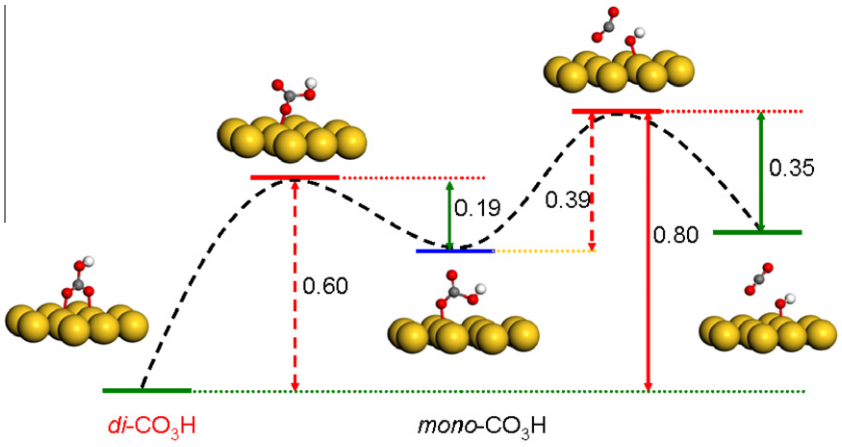

Fig. 12. Schematic illustration of the dissociation reaction of *di*-CO_3H(a) on Au(1 1 1) (from left to right). The reverse reactions (from right to left) represents the deactivation process of Au(1 1 1). The activation energy of each elementary step is also indicated.

We also calculated the kinetics and thermodynamics of the reaction between CO_2 and O(a) to form CO_3(a) on the Au(1 1 1) surface. The reaction of $CO_2 + O(a) \rightarrow CO_3(a)$ proceeds with an activation energy of 0.79 eV and a reaction enthalpy of 0.28 eV, whereas the reverse decomposition reaction of $CO_3(a) \rightarrow CO_2 + O(a)$ proceeds with an activation energy of 0.51 eV and a reaction enthalpy of −0.28 eV (Table 2). This indicates that in the view of both kinetics and thermodynamics, the decomposition reaction of $CO_3(a) \rightarrow CO_2 + O(a)$ is more favored than the reaction of $CO_2 + O(a) \rightarrow CO_3(a)$ at low reaction temperatures, namely, CO_3(a) is not likely to be the poison on the Au surface in low-temperature CO oxidation.

5. Conclusions

Employing Au/SiO_2 inert in catalyzing CO oxidation at temperatures below 150 °C, we have successfully elucidated the influence of hydroxyls on the intrinsic activity of Au nanoparticles in CO oxidation both experimentally and theoretically. Hydroxyls can induce the activation of O_2 on "inert" Au nanoparticles and thus their activity in catalyzing CO oxidation at room temperature. The DFT theoretical calculation results reveal the determining role of COOH(a) in hydroxyls-induced activation of O_2 and catalytic activity of the Au(1 1 1) surface in low-temperature CO oxidation. *di*-CO_3H(a) whose formation is thermodynamically favorable at low reaction temperatures is identified to be the poison leading to the deactivation of $Au/NaOH/SiO_2$ catalysts in low-temperature CO oxidation. These results provide novel insights into the role of hydroxyls in the catalytic activity of Au catalysts and advance the fundamental understanding of oxidation reactions catalyzed by Au catalysts.

Acknowledgments

This work was financially supported by National Natural Science Foundation of China (Grant 20973161), the Ministry of Science and Technology of China (2010CB923302), the MOE program for PCSIRT (IRT0756), and the MPG-CAS partner group program.

References

[1] M. Haruta, N. Yamada, T. Kobayashi, S. Iijima, J. Catal. 115 (1989) 301.
[2] A.S.K. Hashmi, G.J. Hutchings, Angew. Chem. Int. Ed. 45 (2006) 7896.
[3] M. Haruta, M. Daté, Appl. Catal. A 222 (2001) 427.
[4] R. Meyer, C. Lemire, K.Sh. Shaikhutdinov, H.-J. Freund, Gold Bull. 37 (2004) 72.
[5] M.S. Chen, D.W. Goodman, Acc. Chem. Res. 39 (2006) 739.
[6] M.C. Kung, R.J. Davis, H.H. Kung, J. Phys. Chem. C 111 (2007) 11767.
[7] Z.Q. Jiang, W.H. Zhang, L. Jin, X. Yang, F.Q. Xu, J.F. Zhu, W.X. Huang, J. Phys. Chem. C 111 (2007) 12434.
[8] H. Falsig, B. Hovalbæk, I.S. Kristensen, T. Jiang, T. Bligaard, C.H. Christensen, J.K. Nørskov, Angew. Chem. Int. Ed. 47 (2008) 4836.
[9] J.L. Gong, C.B. Mullins, Acc. Chem. Res. 42 (2009) 1063.
[10] G.C. Bond, C. Louis, D.T. Thompson, Catalysis by Gold, Imperial College Press, London, 2006.
[11] E.D. Park, J.S. Lee, J. Catal. 186 (1999) 1.
[12] M. Daté, M. Haruta, J. Catal. 201 (2001) 221.
[13] M. Daté, M. Okumura, S. Tsubota, M. Haruta, Angew. Chem. Int. Ed. 43 (2004) 2129.
[14] C.K. Costello, M.C. Kung, H.-S. Oh, Y. Wang, H.H. Kung, Appl. Catal. A 232 (2002) 159.
[15] C.K. Costello, J.H. Yang, H.Y. Law, Y. Wang, J.-N. Lin, L.D. Marks, M.C. Kung, H.H. Kung, Appl. Catal. A 243 (2003) 15.
[16] H.H. Kung, M.C. Kung, C.K. Costello, J. Catal. 216 (2003) 425.
[17] M.A. Sanchez-Castillo, C. Couto, W.B. Kim, J.A. Dumesic, Angew. Chem. Int. Ed. 43 (2004) 1140.
[18] W.B. Kim, G.J. Rodriguez-Rivera, S.T. Evans, T. Voitl, J.J. Einspahr, P.M. Voyles, J.A. Dumesic, J. Catal. 235 (2005) 327.
[19] J.T. Calla, R.J. Davis, Ind. Eng. Chem. Res. 44 (2005) 5403.
[20] S.T. Daniells, M. Makkee, J.A. Moulijn, Catal. Lett. 100 (2005) 39.
[21] M.A. Debeila, R.P.K. Wells, J.A. Anderson, J. Catal. 239 (2006) 162.
[22] W.C. Ketchie, M. Murayama, R.J. Davis, Top. Catal. 44 (2007) 307.
[23] F. Romero-Sarria, A. Penkova, L.M. Martinez, T.M.A. Centeno, K. Hadjiivanov, J.A. Odriozola, Appl. Catal. B 84 (2008) 119.
[24] J. Dobrosz-Gómez, I. Kocemba, J.M. Rynkowski, Catal. Lett. 128 (2009) 297.
[25] G.M. Veith, A.R. Lupini, N.J. Dudney, J. Phys. Chem. C 113 (2009) 269.
[26] G.C. Bond, D.T. Thompson, Gold Bull. 33 (2000) 41.
[27] T.S. Kim, J.L. Gong, R.A. Ojifinni, J.M. White, C.B. Mullins, J. Am. Chem. Soc. 128 (2006) 6282.
[28] R.A. Ojifinni, N.S. Froemming, J.L. Gong, M. Pan, T.S. Kim, J.M. White, G. Henkelman, C.B. Mullins, J. Am. Chem. Soc. 130 (2008) 6801.
[29] R.G. Quiller, T.A. Baker, X. Deng, M.E. Colling, B.K. Min, C.M. Friend, J. Chem. Phys. 129 (2008) 064702.
[30] A. Bongiorno, U. Landman, Phys. Rev. Lett. 95 (2005) 106102.
[31] L.M. Liu, B. McAllister, H.Q. Ye, P. Hu, J. Am. Chem. Soc. 128 (2006) 4017.
[32] K. Qian, W.X. Huang, Z.Q. Jiang, H.X. Sun, J. Catal. 248 (2007) 137.
[33] K. Qian, W.X. Huang, J. Fang, S.S. Lv, B. He, Z.Q. Jiang, S.Q. Wei, J. Catal. 255 (2008) 269.
[34] K. Qian, H.X. Sun, W.X. Huang, J. Fang, S.S. Lv, B. He, Z.Q. Jiang, S.Q. Wei, Chem. Euro. J. 14 (2008) 10595.
[35] K. Qian, S.S. Lv, X.Y. Xiao, H.X. Sun, J.Q. Lu, M.F. Luo, W.X. Huang, J. Mol. Catal. A 306 (2009) 40.
[36] K. Qian, J. Fang, W.X. Huang, B. He, Z.Q. Jiang, Y.S. Ma, S.Q. Wei, J. Mol. Catal. A 320 (2010) 97.
[37] K. Qian, Z.Q. Jiang, W.X. Huang, J. Mol. Catal. A 264 (2007) 26.
[38] B. Delley, J. Chem. Phys. 113 (2000) 7756.
[39] J.P. Perdew, K. Burke, M. Ernzerhof, Phys. Rev. Lett. 77 (1996) 3865.
[40] N. Govind, M. Petersen, G. Fitzgerald, D. King-Smith, J. Andzelm, Comp. Mater. Sci. 28 (2003) 250.
[41] T.F. Moulder, W.F. Stickle, P.E. Sobol, K.D. Bomben, Handbook of X-ray Photoelectron Spectroscopy, Perkin Elmer, Eden Prairie, Minnesota, 1992. p. 34–242.
[42] N. Weiher, E. Bus, L. Delannoy, C. Louis, D.E. Ramaker, J.T. Miller, J.A. van Bokhoven, J. Catal. 240 (2006) 100.
[43] A. Pantelouris, G. Küper, J. Hormes, C. Feldmann, M. Jansen, J. Am. Chem. Soc. 117 (1995) 11749.
[44] B. Solsona, M. Conte, Y. Cong, A. Carley, G. Hutchings, Chem. Commun. 18 (2005) 2351.
[45] W.H. Zhang, Z.Y. Li, Y. Luo, J.L. Yang, Chin. Sci. Bull. 54 (2009) 1973.
[46] H.Y. Su, M.M. Yang, X.H. Bao, W.X. Li, J. Phys. Chem. C 112 (2008) 17303.
[47] S.D. Senanayake, D. Stacchiola, P. Liu, C.B. Mullins, J. Hrbek, J.A. Rodriguez, J. Phys. Chem. C. 113 (2009) 19536.
[48] Y. Du, N.A. Deskins, Z. Zhang, Z. Dohnálek, M. Dupuis, I. Lyubinetsky, J. Phys. Chem. C 113 (2009) 666.
[49] J. Matthiesen, S. Wendt, J.Ø. Hansan, G.K.H. Madsen, E. Lira, P. Galliker, E.K. Vestergaard, R. Schaub, E. Lægsgaard, B. Hammer, F. Besenbacher, ACS NANO 3 (2009) 517.
[50] H.C. Ham, G.S. Hwang, J. Han, S.W. Nam, T.H. Lim, J. Phys. Chem. C 113 (2009) 12943.
[51] J.A. Rodriguez, S. Ma, P. Liu, J. Hrbek, J. Evans, M. Pérez, Science 318 (2007) 1757.
[52] L.Y. Yeung, M. Okumura, J.T. Paci, G.C. Schatz, J. Zhang, T.K. Minton, J. Am. Chem. Soc. 131 (2009) 13940.